Journal of New Technology and Materials
JNTM
Vol. 02, N°01 (2012)07-12

OEB Univ. Publish. Co.

Transmission Line Matrix: A Tool for Modeling Thermo-Electric properties of Materials and Devices

A. Saidane*, S. Mimouni and R. Houcine
CaSiCCE Laboratory, ENSET-Oran, B.P 1523 M'Naouer-Oran, Algeria
** Email: saidaneaek@yahoo.com*
Received: Dec 29, 2011; accepted as plenary talk of NMCA2011

Abstract

Transmission-Line-Matrix (TLM) method, originally developed in 1971 as a numerical technique for modeling electromagnetic wave propagation, has since been established as a powerful technique to study diffusion problems, vibration, heat transfer, electromagnetic compatibility, radar, etc. The TLM method is a time and space discrete method that solves field problems using their circuit equivalent. It assembles a lattice of discrete points in space as one-dimensional lines and defines the transmission matrix between lattice points, so that successive calculations can be performed. The physical variable is modeled as a sequence of voltage pulses travelling through this network of transmission lines. The TLM routine operates on the travelling, scattering, and connecting of these pulses in the network. The transmission lines in the model act as delay lines, with the node impulse population being the discrete solution at each time step.

TLM is a discrete model which can be solved exactly since approximations are only introduced at the discretisation stage. This is to be contrasted with the traditional approach in which an idealized continuous model is first obtained and then this model is solved approximately. It main advantages are that, it is intuitive and can be simply formulated, explicit, unconditionally stable since it is a passive network which is solved exactly, can be used to model arbitrary and complex structures, inhomogeneous media can be modeled very conveniently, and the impulse response and time domain performance of the system can be obtain straightforwardly.

TLM method is used to model self-heating in various two electronic devices and structures: AlGaN/GaN power transistors and insulated gate bipolar transistor (IGBT) modules. Results show that the method is well suited for understanding heat management in microelectronic devices and gives insights for future designs.

Key words *TLM ; Modeling ; Self-heating ; power transistors ; IGBT modules*

1. Introduction

Transmission-Line-Matrix (TLM) method, originally developed in 1971 as a numerical technique for modeling electromagnetic wave propagation [1], has since been established as a powerful technique to study diffusion problems [2-4], vibration [5,6], heat transfer [7,8], electromagnetic compatibility [9], radar [10], etc. It is based on Huygens principle and could be used for modeling any phenomena which obeys this principle. It is a time and space discrete method that solves field problems using their electrical circuit equivalent. It assembles a lattice of discrete points in space connected by transmission lines and defines the transmission matrix between lattice points, so that successive calculations can be performed. Transmission-lines are considered as distributed models of capacitors, inductors and resistors. The user therefore has a good grasp of the properties and behavior of the model, the nature and significance of errors and the manner in which material properties may be introduced. The physical variable is modeled as a sequence of voltage pulses travelling through this network of transmission lines to become incident simultaneously on all parts of all nodes. These incident pulses are scattered instantaneously into reflected pulses which, during the time step Δ, travel along link transmission lines to become incident upon neighboring nodes. The TLM routine operates on the travelling, scattering, and connecting of these pulses in the network. The transmission lines in the model act as delay lines, with the node impulse population being the discrete solution at each time step.

TLM is a discrete model which can be solved exactly since approximations are only introduced at the discretisation stage. This is to be contrasted with the traditional approach in which an idealized continuous model is first obtained and then this model is solved approximately. It main advantages are that, it is intuitive and can be simply formulated, explicit, unconditionally stable since it is a passive network which is solved exactly, can be used to model arbitrary and complex structures. Inhomogeneous media can be modeled very conveniently, and the impulse response and time domain performance of the system can be obtain straightforwardly.
In this communication, the TLM method is explained and used to model self-heating in various electronic devices and structures. Results show that the method is well suited for understanding heat management in microelectronic devices and gives insights for future devices designs.

2. TLM model

To obtain rise in temperature of device structure, we solve the heat-flow nonlinear equation:

$$\nabla\left[k_t(T)\nabla T\right] + H(x,y,z) = \rho C_p \frac{\partial T}{\partial T} \qquad (1)$$

where T(x, y, z, t) is temperature function and H(x, y, z, t) is heat generation rate per unit volume; ρ is density of solid; Cp is specific heat and k_t is thermal conductivity.
This differential equation is discretized when a physical process is simulated with a conventional numerical method. This is not the case with TLM method, which is intrinsically a

discrete approach that models a physical process directly. Its algorithm preserves physical significance of phenomenon under investigation [2].

It is known that a pulse on a transmission line obeys Maxwell's curl equations for propagation in a lossy medium, which leads to the telegrapher's equation [4]:

$$\nabla^2 \Phi = 2\alpha R_d C_d \frac{\partial \Phi}{\partial t} + \alpha L_d C_d \frac{\partial^2 \Phi}{\partial t^2} \qquad (2)$$

where $\Phi(x, y, z, t)$ is potential and L_d, C_d and R_d are inductance, capacitance, and resistance per unit of length, respectively. Constant α = 1, 2 or 3 for one, two and three dimensions. Equation (2) is without loss if R_d=0 and becomes consequently identical to a wave equation. On the other hand, if $R_d \neq 0$, then the equation describes an attenuated wave. When the first time-derived term on the right-hand side of equation (2) dominates the second time-derived term, one can establish equivalence with the thermal diffusion process described by equation (1). Hence, one practical application of the TLM method is its use to model physical problems where electrical/thermal analogies are possible.

The TLM method operates on a grid structure and replaces each node with an equivalent circuit of transmission lines. An equivalent TLM node of the structure under investigation is shown in Fig.1. When a pulse is sent on a transmission line element, the potential F obeys the telegrapher's equation (2). In the TLM, data in the form of potential or current values are represented by delta pulses. It is also supposed that all these pulses move in the network in synchronism. In Fig.1, the current generator I is used to model the generation of heat within the device. It represents the power injected in each node (x, y, z) in the active area. Electrical resistance and localized capacitance, in a transmission line without loss, model thermal resistance and heat capacity of the material, respectively. They are given by the following equations:

$$R_X = \frac{dx}{2K_t dydz}, \quad R_Y = \frac{dy}{2K_t dxdz}, \quad R_Z = \frac{dz}{2K_t dydx}$$
$$Z = \frac{\alpha \Delta t}{\rho C_p \Delta x \Delta y \Delta z} \qquad (3)$$

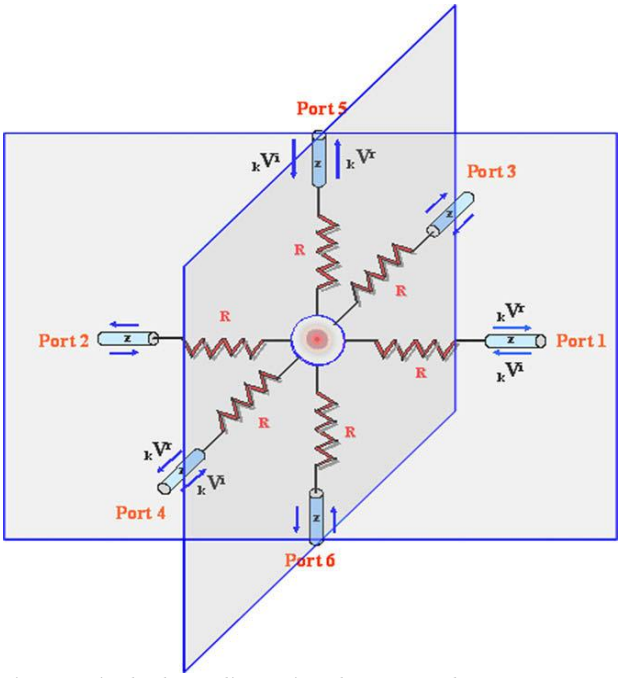

Fig.1. A single three-dimensional TLM node.

An iterative method is used to obtain nodal potential (temperature) resulting from the injection of delta pulses (input heat) in the network after each time step. Indeed, when pulses travel down the transmission lines, they are scattered at nodes, with part of pulse reflected into the same line and the other part transmitted to neighboring nodes. Hence, local nodes potentials provide an exact solution to equation (2) at each time step. Directions of pulses on each numbered port are shown on Fig.1. These pulses are labeled ${}_kV_j^{i,r}$ with j indicating the direction and k the k^{th} iteration.

Applying Thevenin and Millman theorems to equivalent electric circuit of a TLM node, nodal potential V at the k^{th} iteration can be derived:

$${}_kV = \left[\frac{2\left({}_kV_1^i + {}_kV_2^i\right)}{R_X + Z} + \frac{2\left({}_kV_3^i + {}_kV_4^i\right)}{R_Y + Z} + \frac{2\left({}_kV_5^i + {}_kV_6^i\right)}{R_Z + Z} + I \right] \frac{1}{Y} \qquad (4)\text{ICLE}$$

$$Y = \frac{1}{\frac{1}{R_X + Z} + \frac{1}{R_Y + Z} + \frac{1}{R_Z + Z}}$$

where $Z=3\Delta t/C$ is the characteristic impedance.

Reflected pulses at a node, indicated by superscript r, are calculated according to:

$${}_kV_{1,2}^r = \frac{Z\ {}_kV + \left(R_X - Z\right){}_kV_{1,2}^i}{R_X + Z},$$
$${}_kV_{3,4}^r = \frac{Z\ {}_kV + \left(R_y - Z\right){}_kV_{3,4}^i}{R_y + Z}, \qquad (5)$$
$${}_kV_{5,6}^r = \frac{Z\ {}_kV + \left(R_z - Z\right){}_kV_{5,6}^i}{R_z + Z}$$

Each pulse takes a time Δt to move down a transmission line joining two neighboring nodes. Reflections at discontinuities, due to impedance mismatch, give incident pulses at $(k+1)^{th}$ iteration:

$${}_{k+1}V_j^i(x, y, z) = \Gamma_j(x, y, z)\,{}_kV_j^r(x, y, z) + \left[1 - \Gamma_j(u, v, w)\right]{}_kV_{j'}^r(u, v, w) \qquad (6)$$

$$with \quad \Gamma_j = \frac{Z(u, v, w) - Z(x, y, z)}{Z(u, v, w) + Z(x, y, z)}$$

Table 1 shows j, j', u, v and w values.

j	j'	u	v	w
1	2	x-1	y	z
2	1	x+1	y	z
3	4	x	y-1	z
4	3	x	y+1	z
5	6	x	y	z-1
6	5	x	y	z+1

Table 1 : j, j', u, v and w values.

Implementation of a TLM routine consists solely of repeated application of equations (4)-(6). TLM simulation algorithm can be accelerated by timestep changes and grid coarsening.

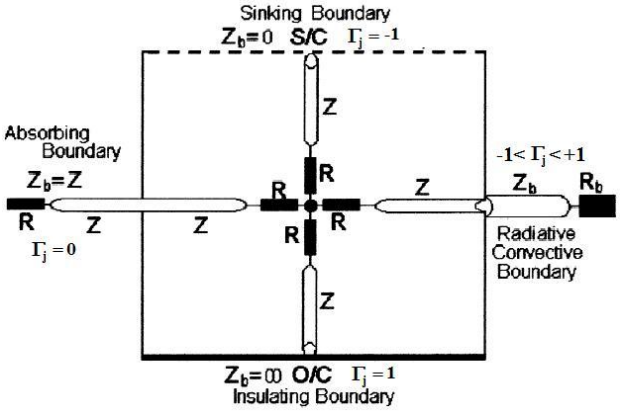

Fig.2 TLM boundary conditions.

Boundary conditions express interaction of system at hand with its surroundings. Boundaries are part of the transport model and thus should be consistent with the description of heat transport inside the medium. A heat sinking boundary corresponds to an electrical short-circuit (S/C) and $\Gamma_j = -1$, thus any incident pulse on the boundary will be returned equal in magnitude but reversed phase. A heat insulating boundary corresponds to an electrical open-circuit (O/C) and $\Gamma_j = 1$, thus any incident pulse on the boundary will be returned equal in magnitude and in phase. A symmetry boundary is represented by an electrical open-circuit in TLM modeling [2,4]. Convective or radiative heat losses at boundaries may be considered as a heat sink and modeled using an appropriate reflection coefficient, Fig.2. A constant heat source boundary, Φ_b, is modeled by taking, at the boundary interface:

$$V_b^i + V_b^r = \Phi_b$$

where V_b^i *and* V_b^r are incident and reflected pulses of the node attached to the source at the surface.

3. Self-heating in AlGaN/GaN power transistors

Gallium nitride (GaN) and its compounds are being established as materials of extreme significance for next generation high-density power devices. Due to their high breakdown voltages, high electron mobility, and high thermal conductivities, these materials allow the fabrication of devices, which can operate at voltages, and temperature ranges beyond the conventional semiconductor materials, such as GaAs and Si. They are used in microwave radar and mobile telecommunications [10,11]. AlGaN/GaN heterostructure field-effect transistors symbolized by HFET, operate at high frequency with a high signal-to-noise ratio. However, operation of these devices is limited by self-heating under pulsed working conditions and other problems associated with high densities of defects. This self-heating makes thermal management a crucial aspect in device-packaging design. Several system-level cooling schemes have been presented for efficient heat dissipation, such as flip-chip bonding, two-phase spray cooling and mounting devices onto high thermal conductivity substrates [12–16].

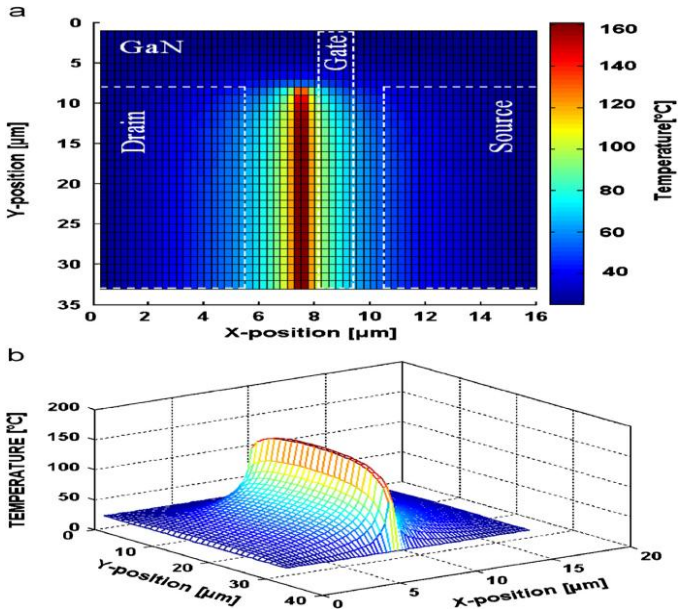

Fig.3 Temperature distribution around active region.

Fig.3a shows the surface temperature of GaN that contains the active zone. A hot-area with a maximum temperature of approximately 160.7°C, located between the source and the drain meadows of the HFET gate, is clearly visible. Fig.3b is a 3D representation of the same surface. It shows a dorsal-like temperature distribution with a peak value near the drain because of the dissymmetry. With this representation of TLM results, one can easily evaluate temperature at each point of device. This represents a great advantage compared with certain measurement techniques such as, infrared (IR) thermography or micro-Raman spectroscopy, where the temperature-measured value is an average taken at a certain thickness of device.

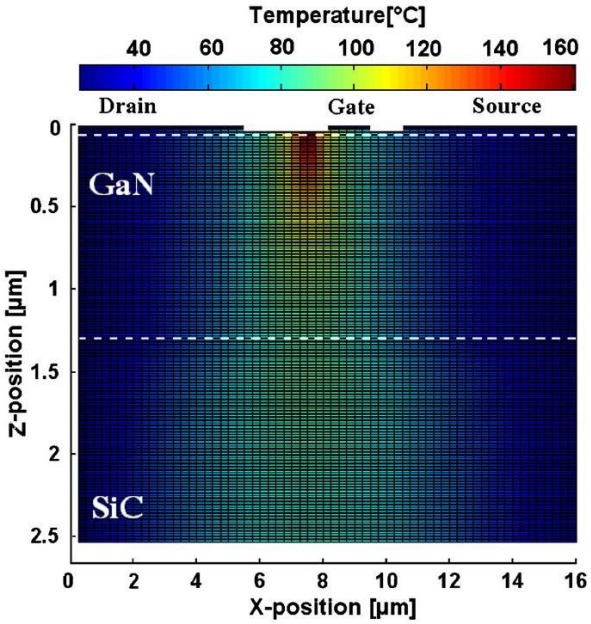

Fig.4 Temperature distribution along the z-axis.

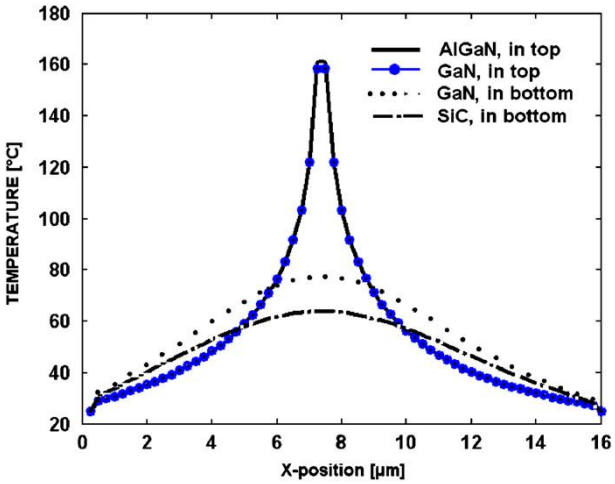

Fig.5 Temperature distribution at various depth levels.

Fig.4 shows temperature distribution along the z-axis and Fig.5 shows temperature distribution along the x-axis at four interface positions: AlGaN layer, AlGaN/GaN, GaN/SiC and SiC/sink. This vertical cut through different device layers gives in-depth information on heat management in each layer. Furthermore, change in slope indicates a change in heat transfer dynamics going from a layer to another. Temperature in the AlGaN layer of the device is higher than that found in the GaN layer [17,18]. But heat does not accumulate at various interfaces, which otherwise would be a problem since it might lead to hot-spot formation. Hence, in comparison with other analysis methods, with TLM one can determine the place and form of hot area with more precision.

4. Electro-thermal analysis of IGBT modules.

Trends in power converter systems are to reduce converter size and to increase switching frequency. Both requirements increase heat generation rates which become a critical issue to study and optimize. This is the case of insulated gate bipolar transistor (IGBT) modules with their high voltage (several kV) and high current (several kA). Here, a thermal analysis of a 1200 A, 3.3 kV IGBT module was investigated and analyzed using Three-Dimensional Transmission Line Matrix (3D-TLM), Fig.6, including measurement and numerical results obtained by other simulators tools as MSC.PATRAN [19], FLOTHERM [20] and LAASTHERM [21]. Thermal simulations were run for various power loads and devices with different heat spreaders such as AlSiC, Cu–Mo, Graphite–Cu and Cu of various thicknesses.

IGBT modules have exhibited different thermal behaviors depending on substrate material used. Materials such as Aluminium Nitride (AlN), Diamond and BeO have particularly good thermal conductivity. These ceramics provide electrical insulation to the underlying base plate, which is usually pressure mounted onto a heat sink by peripheral bolts [22]. The use of ceramic substrates is to decrease self-heating from heat sources localized within IGBT modules.

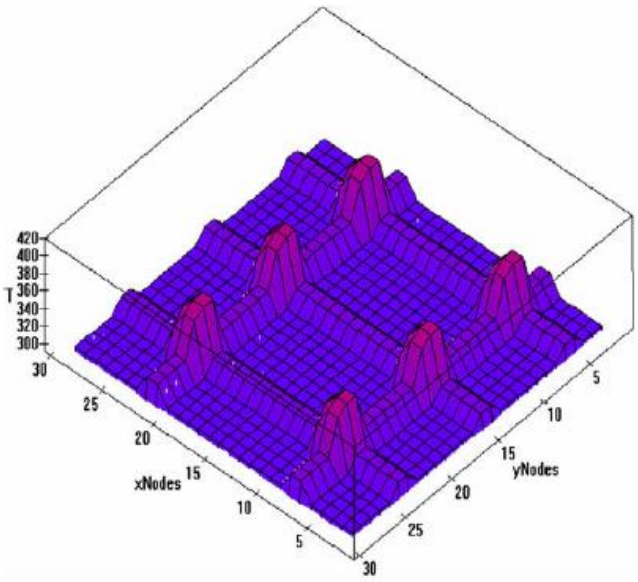

Fig.6 Typical TLM temperature distribution in an IGBT module.

Prediction of temperature rise is important in pulse operation conditions, Fig.7. This temperature profile is obtained with 100 W-step pulses where control signals are generated via a PWM scheme. Temperature rises are calculated using TLM for three load cycles and result is shown in Fig.8. During first load cycle, temperature rise and drop are important, and then thermal gradient decrease with increasing load cycles. Other simulations were performed to show the importance of heat spreaders that are included between the device and its heat sink. Fig.9 shows results for three heat spreaders AlSiC, Cu and CuMo. Thermal transients cross-over occurs at different points in time. The main difference between Cu and CuMo in terms of thermal properties is that Cu has a significantly higher thermal conductivity K and a higher thermal diffusivity than CuMo.

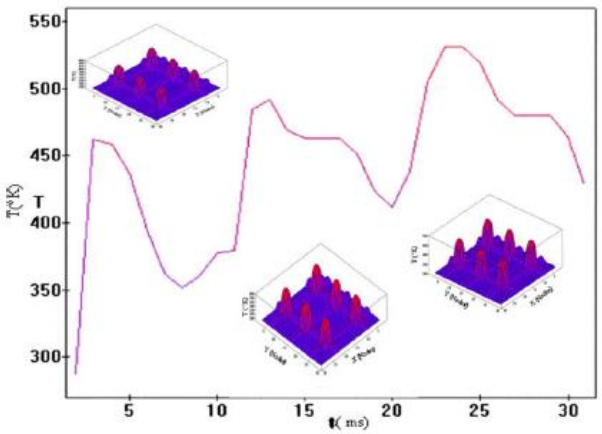

Fig.7 Temperature evolution in pulsed mode.

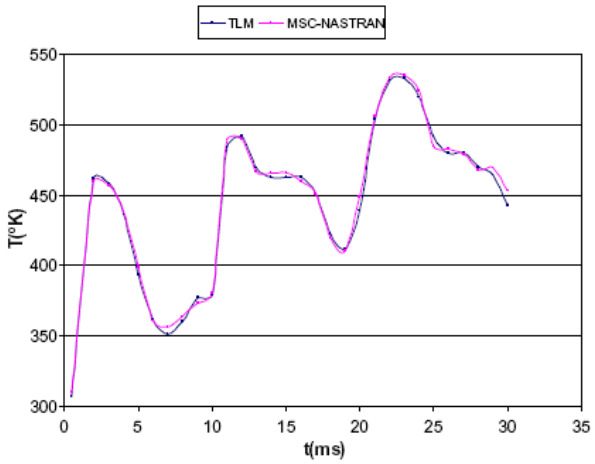

Fig.8 Comparison of TLM and MSC-NASTRAN.

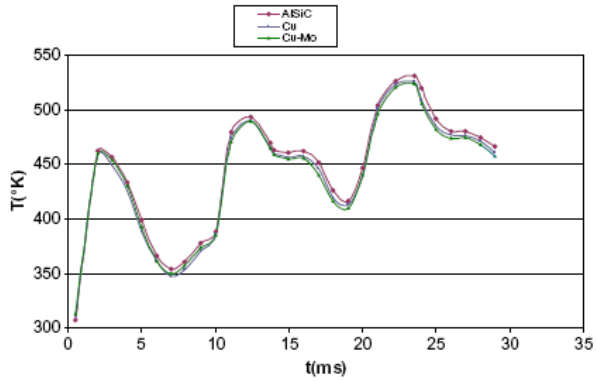

Fig.9 TLM results for 3 different heat spreaders.

Temperature differences are larger in the case of AlSiC spreader, which is associated with higher chip and solder temperatures. Although thermal diffusivity of AlSiC falls between that of Cu and that of CuMo, and its thermal conductivity is less than a half of that of Cu and its specific heat capacity - density product is only a third that of CuMo, chip temperatures were found to be lowest with a Cu spreader and highest with an AlSiC spreader with CuMo yielding intermediate values. This means that the model with the CuMo heat spreader always starts each successive pulse at a lower temperature than the model with a Cu heat spreader. Since the assembly is a layered structure, materials with different CTE can cause the layers of the assembly to warp when subjected to rapid thermal excitation. Therefore, component design should not only take into account thermal and physical problems inherent to chip-to-heat sink assembly, but also interaction issues between layers of heat sink assembly itself. This implies that, as the number of pulses increases, cooling rates of heat sink assembly will play a more important role in ensuring an acceptable overall temperature, as relatively more heat will be dissipated with each successive pulse.

5. Conclusion

The TLM method was applied to study self-heating in AlGaN/GaN device structures and insulated gate bipolar transistor (IGBT) modules. The method is easy to program and gives insights on temperature distribution throughout the device. It allows a better understanding of heat behavior and management at each layer that forms the structure. Absolute temperature determination and precise hot-area size knowledge are very difficult to assess in both HFET devices employing IR micro-thermography or in IGBT interfaces. The TLM can be a good alternative design tool, since it allows the evaluation of temperature at any point of the structure. Its physical resolution depends on the grid used only and complex geometries can be dealt with easily. Some TLM simulations results have been compared with those obtained experimentally using integrated micro-Raman/IR thermography methods or with other modeling methods, and have been found to agree within the bounds set by the resolution required. TLM method will prove handy in the study of heat management of many materials used in semiconductor devices fabrication. TLM has also the advantage upon other numerical methods of being unconditionally stable, one step, can adapt to complex geometries, and simple to program.

References

[1] P.B. Johns, R.L. Beurle, Proceedings of the IEE 118 (1971) 1203.

[2] D. de Cogan, W.J. O'Connor, S. Pulko, Transmission Line Matrix Modelling in Computational Mechanics, Taylor & Francis, CRC Press, London, 2006.

[3] C. Christopoulos, The Transmission-Line Modeling Method (TLM), IEEE Press, New York, 1995.

[4] D. De Cogan, Transmission Line Matrix (TLM) Techniques for Diffusion Applications, Gordon and Breach, 1998.

[5] A. Saleh, P. Blanchfield, , International Journal of Numerical Modeling, 3 (1990) 39.

[6] I.J.G. Scott, D. de Cogan, Journal of Sound and Vibration , 311 (2008) 1213.

[7] A.Amri, A.Saidane, S.Pulko, Computers in Biology & Medicine 41 (2011) 76.

[8] S.Aliouat-Bellia, A.Saidane, A.Hamou, M.Benzohra, J.M.Saiter, Burns 34 (2008) 688.

[9] W.J.R. Hoefer, The transmission line matrix (TLM) method, in: T. Itoh (Ed.), Numerical Techniques for Microwave and Millimeter-Wave Passive Structures, Wiley, 1989.

[9] A.K. Iyer, G.V. Eleftheriades, Applied Physics Letters 92 (2008) 131.

[10] S. Nuttinck, E. Gebara, J. Laskar, M. Harris, IEEE Microw. Mag. 3/1 (2002) 80.

[11] M. Kuzuhara, H. Miyamoto, Y. Ando, T. Inoue, Y. Okamoto, T. Nakayama, Phys. Stat. Sol. A 200/1 (2003) 161.

[12] J.J. Xu, Y.F. Wu, S. Keller, G. Parish, S. Heikman, B.J. Thibeault, U.K. Mishra, R.A. York, IEEE Microw. Guided Wave Lett. 9/7 (1999) 277.

[13] J. Sun, H. Fatima, A. Koudymov, A. Chitnis, X. Hu, H.M. Wang, J. Zhang, G. Simin, J. Yang, M.A. Khan, IEEE Electron. Device Lett. 24/4 (1999) 375.

[14] S.L. Lee, Z.H. Yang, Y. Hsyua, J. Heat Transf. 116 (1994) 167.

[15] S .Heffington, W.Z. Black, A. Glezer., in: Proceedings of International Electronic Packaging Conference, (2001) 779.

[16] J.Y Murthy, C.H Amon, K. Gabriel, P. Kumta, S.C. Yao, . , in: Proceedings of International Electronic Packaging Conference, (2001) 733.

[17] S. Rajasingam, J.W. Pomeroy, M. Kuball, M.J. Uren, T. Martin, D.C. Herbert, K.P. Hilton, R.S. Balmer, IEEE Electron. Device Lett. 25 (7) (2004) 456.

[18] I. Ahmad, V. Kasisomayajula, M. Holtz, J.M. Berg, S.R. Kurtz, C.P. Tigges, A.A. Allerman, A.G. Baca, Appl. Phys. Lett. 86 (17) (2005) 503.

[19] MSC.PATRAN, complete software environment for simulation, (http://www.mscsoftware.com.au/).

[20] ANSYS FLOTHERM, Ansys Inc, (http: / /www.ansys.com).

[21] A. Hamidi, G. Coquerz, R. Lallemand, P. Vales, Microelectron. Reliability J., 38 (1998) 1353.

[22] C.Van Godbold,V. Sankaran, J.L. Hudgins, IEEE Trans. Power Electron. , 12 /1 (1997) 3